Received: 15 August 2019 | Revised: 10 December 2019 | Accepted: 23 December 2019

DOI: 10.1096/fj.201902093R

RESEARCH ARTICLE

THE FASEB JOURNAL

Calcium affects CHP1 and CHP2 conformation and their interaction with sodium/proton exchanger 1

Shuo Liang[1,2] | **Simon Fuchs**[1,2] | **Evgeny V. Mymrikov**[1,3] | **Anja Stulz**[4] | **Michael Kaiser**[4] | **Heiko Heerklotz**[3,4,5,6] | **Carola Hunte**[1,3,6]

[1]Institute for Biochemistry and Molecular Biology, ZBMZ, Faculty of Medicine, University of Freiburg, Freiburg, Germany

[2]Faculty of Biology, University of Freiburg, Freiburg, Germany

[3]CIBSS - Centre for Integrative Biological Signalling Studies, University of Freiburg, Freiburg, Germany

[4]Department of Pharmaceutical Technology and Biopharmacy, University of Freiburg, Freiburg, Germany

[5]Leslie Dan Faculty of Pharmacy, University of Toronto, Toronto, Canada

[6]BIOSS Centre for Biological Signalling Studies, University of Freiburg, Freiburg, Germany

Correspondence
Carola Hunte, Institute for Biochemistry and Molecular Biology, ZBMZ, Faculty of Medicine, CIBSS, University of Freiburg, Stefan-Meier-Strasse 17, Freiburg 79104, Germany.
Email: carola.hunte@biochemie.uni-freiburg.de

Funding information
Deutsche Forschungsgemeinschaft (DFG), Grant/Award Number: SFB 746, Project-ID 403222702 / SFB 1381, Project-ID 278002225 / RTG 2202, under Germanys Excellence Initiative, BIOSS - EXC-294 and under Germanys Excellence Strategy,CIBSS - EXC-2189 - Project-ID 390939984

Abstract

Calcineurin B homologous proteins (CHPs) belong to the EF-hand Ca^{2+}-binding protein (EFCaBP) family. They have multiple important functions including the regulation of the Na^+/H^+ exchanger 1 (NHE1). The human isoforms CHP1 and CHP2 share high sequence similarity, but have distinct expression profiles with CHP2 levels for instance increased in malignant cells. These CHPs bind Ca^{2+} with high affinity. Biochemical data indicated that Ca^{2+} can regulate their functions. Experimental evidence for Ca^{2+}-modulated structural changes was lacking. With a newly established fluorescent probe hydrophobicity (FPH) assay, we detected Ca^{2+}-induced conformational changes in both CHPs. These changes are in line with an opening of their hydrophobic pocket that binds the CHP-binding region (CBD) of NHE1. Whereas the pocket is closed in the absence of Ca^{2+} in CHP2, it is still accessible for the dye in CHP1. Both CHPs interacted with CBD in the presence and absence of Ca^{2+}. Isothermal titration calorimetry (ITC) analysis revealed high binding affinity for both CHPs to CBD with equilibrium dissociation constants (K_Ds) in the nanomolar range. The K_D for CHP1:CBD was not affected by Ca^{2+}, whereas Ca^{2+}-depletion increased the K_D 7-fold for CHP2:CBD showing a decreased affinity. The data indicate an isoform specific regulatory interaction of CHP1 and CHP2 with NHE1.

KEYWORDS

calcineurin B homologous proteins, Ca^{2+} signaling, EF-hand Ca^{2+}-binding proteins, NHE1, protein-protein interaction

Abbreviations: CaM, calmodulin; CBD, CHP-binding region of sodium/proton exchanger 1 (residues 503 to 545); CHP, calcineurin B homologous protein; CV, column volumes; EFCaBPs, EF-hand Ca^{2+}-binding proteins; FPH assay, fluorescent probe hydrophobicity assay; ITC, isothermal titration calorimetry; MBP, maltose-binding protein; MST, microscale thermophoresis; NHE1, sodium proton exchanger 1; PAGE, polyacrylamide gel electrophoresis.

1 | INTRODUCTION

Calcineurin B homologous proteins (CHPs) belong to the EF-hand Ca^{2+}-binding protein (EFCaBP) family and share a high amino acid sequence similarity with calcineurin B.[1] Among their multiple important functions is the regulation of the Na^+/H^+ exchanger 1 (NHE1), which is required for control of intracellular pH and cell volume.[1] The CHP subfamily consists of isoforms CHP1, CHP2, and CHP3. Whereas CHP1 and CHP3 are ubiquitously present in the human body,[2] CHP2 is mostly occurring in highly proliferating cells, for example, in intestine, testis and skin, with a significantly increased level in malignant cells.[2,3] The primary structures of CHP1 and CHP2 are very similar (75 % similarity), whereas that of CHP3 differs (30% and 42% similarity to CHP1 and CHP2, respectively).[1] Structures of CHP1 and CHP2 were determined in complex with a target peptide derived from human NHE1.[4,5] Both CHPs share a similar ternary structure with two distinct globular parts (N- and C-lobe), connected with a flexible linker (CHP-loop).[4,5] Each lobe contains two EF-hand motifs, but only the EF-hands in the C-lobe (EF-3 and EF-4) are functional.[1,6,7] The target peptide is bound in a hydrophobic pocket enclosed by these two lobes. This binding mode is a common feature of EFCaBPs.[8]

Usually, EFCaBPs undergo a conformational change upon Ca^{2+}-binding to the EF-hands.[9,10] Calmodulin (CaM) is a classic example. It adopts an open conformation in Ca^{2+}-bound state, in which the target proteins can bind to hydrophobic patches in a four-helix bundle.[11] In the apo-state, CaM is present in a closed conformation.[11] For CHP1 and CHP2, the effect of Ca^{2+}-binding on conformational state and downstream regulatory activity is controversial. Ca^{2+}-induced conformational changes of rat CHP1, which was then called p22, were detected by a little mobility shift in clear native polyacrylamide gel electrophoresis (CN-PAGE).[12] Variants of CHP1 and CHP2 with impaired Ca^{2+}-binding sites showed decreased electrophoretic mobility compared to wild-type proteins and a Ca^{2+}-induced conformational change was suggested.[6,7] Yet, the assay was performed in denaturing conditions thus not reflecting the native state of the proteins. Moreover, the gel-shift was not observed in a direct comparison of Ca^{2+}-free and Ca^{2+}-bound forms of wild-type human CHP1.[13] In contrast, Ca^{2+}-induced conformational changes were clearly shown for CHP3 by monitoring intrinsic tryptophan fluorescence and far-UV circular dichroism spectra.[14] Thus, direct experimental evidence for Ca^{2+}-induced conformational changes in CHP1 and CHP2 using biochemical or structural approaches was lacking so far.

The effect of Ca^{2+} on the structure and function of CHP1 and CHP2 is debated. Pang and coworkers proposed that EF-hands 3 and 4 of CHP1 and CHP2 are always present in Ca^{2+}-bound state in vivo, even under resting Ca^{2+} concentrations (~100 nM), as high Ca^{2+} binding affinities were determined for these CHPs in vitro (<100 nM).[6,7] The authors concluded that Ca^{2+}-coordination by EF-3 and EF-4 should be only important for structural stabilization and the conformational states of CHP1 and CHP2 should not be affected by Ca^{2+}-signals.[6,7] In contrast, several studies reported a Ca^{2+}-modulated interaction of CHP1 and CHP2 with their targets, suggesting that these CHPs might act as Ca^{2+}-sensor proteins.[1] For instance, Ca^{2+} is required for the interaction between rat CHP1 and the motor protein Kinesin-like protein 1Bß2 (KIF1Bß2)[15]; CHP1 inhibits death-associated protein kinase-related apoptosis inducing protein kinase 2 (DRAK2) in a Ca^{2+}-dependent manner[16]; Ca^{2+} is important for the activation of calcineurin A by CHP2[17] and for the complex formation of CHP2 with the cytoplasmic region (amino acid residues 515-545) of NHE1.[7]

The interaction between CHPs and NHE1 is of particular interest, as NHE1 is an important regulator of intracellular pH homeostasis and cell volume.[18] CHPs are crucial for the trafficking of NHE1 as well as for its stabilization on the plasma membrane.[13,19] A recessive mutation in *CHP1* causes ataxia and degeneration of cerebellar mouse Purkinje cells.[20] Recently, it was described that the genetic deletion of Lys19 in CHP1 also leads to the development of human cerebellar ataxia.[21] Interestingly, a similar pathological state was observed in patients carrying mutations of NHE1.[22,23]

All CHPs bind to the same amphipathic helix in the regulatory C-terminal domain of NHE1 (residues 503-545, designated as CBD or CHP-binding region).[13,24] Conceptually, CHPs could compete for binding to CBD when simultaneously expressed in the same cell. CHP1 and CHP3 were both shown to be present in mouse Purkinje cells. High CHP1 levels in young animals decreased upon aging, whereas the level of CHP3 increased.[20] In malignant cells, increased CHP2 levels along with a basal level of CHP1 were reported.[2,3] Quantitative characterization of the interaction between CHP3 and CBD by isothermal titration calorimetry (ITC) revealed a high binding affinity with an equilibrium dissociation constant (K_D) of 3 nM,[24] but comparable data were missing for the interaction of CHP1 and CHP2 with CBD.

First indications for an effect of Ca^{2+}, on the interaction of CHPs with NHE1, were derived from biochemical studies. Initially, NHE1 interaction with CHP1 was shown to be Ca^{2+}-independent based on co-localization and co-immunoprecipitation experiments.[5,13] Later, Pang et al. stated that complex formation between CHP1 and NHE1 was reduced upon Ca^{2+}-depletion, but could still be detected.[6] Similarly, Ca^{2+}-depletion decreased complex formation between CHP2 and NHE1 in co-immunoprecipitation experiments.[7] It was not known whether Ca^{2+} induces a conformational change of CHP1 and CHP2 that could modulate target binding. Also,

quantitative analysis of the effect of Ca^{2+} on the interaction of NHE1 with CHP1 and CHP2 was lacking. Biochemical and biophysical characterization of the interaction of CHP1 and CHP2 with NHE1 and of Ca^{2+} effects on this interaction and on CHPs is important to understand the regulatory mechanisms of NHE1 in detail.

2 | MATERIALS AND METHODS

All column materials if not otherwise noted were obtained from GE Healthcare, Chicago, Illinois, USA.

2.1 | Cloning and mutagenesis

The coding sequences of human CHP1 (GC15P04123, Gene ID 11261, UniProtKB ID Q99653) and human CHP2 (GC16P023824, Gene ID 63928, UniProtKB ID O423745) were cloned into the vector pBADM-11 (EMBL-AG, Heidelberg, Germany), downstream of the sequence for N-terminal hexa-histidine tag and Tobacco Etch Virus endopeptidase (TEV) cleavage site (Glu-Asn-Leu-Tyr-Phe-Gln\Gly) to yield the protein product Met-Lys-6xHis-Pro-Met-Ser-Asp-Tyr-Asp-Ile-Pro-2xThr-Glu-Asn-Leu-Tyr-Phe-Asn-Gly-Ala-CHP1_HUMAN$_{2\text{-}195}$, and the protein product Met-Lys-6xHis-Pro-Met-Ser-Asp-Tyr-Asp-Ile-Pro-2xThr-Glu-Asn-Leu-Tyr-Phe-Gln-Gly-Ala-CHP2_HUMAN$_{2\text{-}196}$. The resulting plasmids were designated as pBADM11-*CHP1* and pBADM11-*CHP2*.

2.2 | Protein production and purification

Expression cultures of 200 mL 2xYT medium (100 mg/mL carbenicillin [2xYT^{carb}]) were started with single colonies of *E. coli* BL21(DE3) cells transformed with pBADM11-*CHP1*, which had been grown overnight at 37°C on Luria-Bertani (LB)^{carb}-agar media. The pre-cultures were grown at 37°C (220 rpm) overnight and then added to 6 × 2 l 2×YT^{carb} medium to yield $OD_{600} = 0.05$. The main cultures were incubated at 37°C (180 rpm) and protein production was induced with 0.02% (w/v) L-arabinose at an $OD_{600} = 0.5\text{-}0.6$. After 5 hours incubation at 25°C, cells were harvested by centrifugation and the cell sediment was stored at −80°C. For cell disruption, about 30 *g* cell sediment was thawed and resuspended in 150 mL lysis buffer (1×PBS: 137 mM NaCl, 2.7 mM KCl, 12 mM sodium phosphate, 20 mM imidazole, 1 mM EDTA; pH 7.5) with 1 mM Pefabloc (Carl Roth GmbH, Karlsruhe, Germany). The cell suspension was passaged three times through the cell disruptor (Constant Systems Ltd., Daventry, UK). Cell debris was removed by centrifugation (4°C, 35 000 *g*, 30 minutes). The cleared cell lysate was loaded onto an immobilized metal affinity chromatography (IMAC) column (5 mL HisTrap FF) pre-equilibrated with buffer A1 (20 mM sodium phosphate, 500 mM NaCl; pH 6.0) with 20 mM imidazole. After loading, five column volumes (CV) of buffer A1, five CV of buffer B1 (20 mM sodium phosphate, 500 mM NaCl; pH 4.7) and five CV of buffer A1 were applied. CHP1 was eluted with buffer A1 with 500 mM imidazole. The eluted fractions (10 mL) were pooled, diluted with buffer (20 mM sodium phosphate, 0.5 mM EGTA, 0.5 mM DTT; pH 6.0) in a 1:4 ratio and TEV-protease was added to a final concentration of 0.017 mg/mL. The sample was dialyzed against buffer (20 mM Tris-HCl, 20 mM NaCl, 0.5 mM EDTA, 0.5 mM DTT; pH = 8.5) overnight at 4°C. The dialyzed sample was centrifuged at 4°C 35 000 *g* for 30 minutes and the supernatant was loaded onto an IMAC column (5 mL HisTrap FF) pre-equilibrated with buffer C1 (20 mM Tris-HCl, 20 mM NaCl; pH 8.5). The flow through was pooled and loaded onto an anion-exchange chromatography column (5 mL HiTrap DEAE FF) pre-equilibrated with buffer C1. The protein was eluted with a gradient from 0 to 1 M NaCl. The eluted fractions were pooled and concentrated by spin filtration (Amicon Spin concentrator, 10 000 MWCO, Merck Millipore, Burlington, USA). The concentrated protein was loaded onto a gel-filtration column (HiLoad Superdex 75 16/60) with 20 mM Tris-HCl, 150 mL NaCl (pH 8.5) used for equilibration and separation. The eluted pure protein was concentrated and stored in aliquots in the presence of 1 M sucrose at −80°C. We obtained 3 mg per liter cell culture of purified CHP1.

Production of CHP2 was performed essentially as described for CHP1 by using the plasmid pBADM11-*CHP2*. For cell disruption, about 35 *g* cell sediment was thawed and resuspended in 175 mL lysis buffer (20 mM HEPES, 500 mM NaCl, 20 mM imidazole, 1 mM EDTA, 10% glycerol, 1 mM DTT; pH 7.2) with 1 mM Pefabloc (Carl Roth GmbH). The cell disruption and cell debris removal were performed as described above. The cleared cell lysate was loaded onto a 5 mL IMAC column (HisTrap FF) pre-equilibrated with buffer A2 (20 mM HEPES, 500 mM NaCl, 20 mM imidazole; pH 7.2). After loading, 40 CV of buffer A2 was applied to wash out unspecific bound proteins. CHP2 was eluted with a gradient from 20 to 300 mM imidazole. The eluted fractions were pooled, diluted with buffer B2 (20 mM HEPES, 0.5 mM EGTA, 0.5 mM DTT; pH 7.2) in a 1:3 ratio. TEV-protease (0.013 mg/mL final concentration) was added. The sample was dialyzed against buffer B2 with 50 mM NaCl overnight at 4°C. The dialyzed sample was centrifuged at 4°C with 35 000 *g* for 30 minutes and the supernatant was supplemented with imidazole to a final concentration of 66 mM. The sample was then loaded onto an IMAC column (5 mL HisTrap FF) pre-equilibrated with buffer A2. The flow through was pooled, supplemented with $CaCl_2$ to a final concentration of 11 mM, and loaded onto a

hydrophobic interaction chromatography (HIC) column (2 × 1 mL, Butyl Sepharose HP) pre-equilibrated with buffer C2 (20 mM HEPES, 150 mM NaCl; pH 7.2) with 10 mM $CaCl_2$. The protein was eluted with buffer C2 with 10 mM EGTA. The eluted fractions were pooled and diluted with buffer C2 with 10 mM $MgCl_2$ in a 1:4 ratio and then concentrated by spin filtration as described above. The concentrated protein was loaded onto a gel-filtration column (HiLoad Superdex 75 16/60), with buffer C2 with 10 mM $MgCl_2$ used for equilibration and separation. The eluted pure protein was concentrated and stored in aliquots in the presence of 1 M sucrose at −80°C. We obtained 2.6 mg per liter cell culture of purified CHP2.

Production and purification of human CaM and maltose-binding protein (MBP)-CBD was performed essentially as described earlier.[24] The production and purification of CHP3 was performed with HIC and gel filtration as described for other EFCaBPs.[25]

The protein concentration was determined spectroscopically with NanoDrop 2000 spectrophotometer (Thermo Fisher Scientific, Waltham, USA) or with the Cary 4000 UV-vis spectrophotometer for the microscale thermophoresis (MST) and ITC measurements (Agilent technologies, Mulgrave, Australia) using calculated extinction coefficients (ExPaSy: https://web.expasy.org/protparam/protparam-doc.html) of $\varepsilon_{280} = 2980\ M^{-1}\ cm^{-1}$ (CHP1; 22.5 kDa), $\varepsilon_{280} = 4470\ M^{-1}cm^{-1}$ (CHP2; 22.5 kDa), $\varepsilon_{280} = 11\ 460\ M^{-1}cm^{-1}$ (CHP3; 24.6 kDa), $\varepsilon_{280} = 2980\ M^{-1}cm^{-1}$ (CaM; 18.2 kDa), and $\varepsilon_{280} = 69\ 330\ M^{-1}cm^{-1}$ (MBP-CBD; 48.6 kDa).

2.3 | Denaturing and native PAGE

Protein samples were separated by sodium dodecyl sulfate (SDS)-PAGE using a 12% Bis-Tris Mini Gel system (NuPAGE, Invitrogen Life Technologies, Carlsbad, USA) at a constant voltage of 100 V for 3.5 hours. The running buffer was composed of 0.1% SDS (w/v), 50 mM MES, 50 mM Tris-HCl, 1 mM EDTA; pH 7.3. 20 µL of each 20 µM protein sample was mixed with 20 µL 2X lithium dodecyl sulfate (LDS) sample buffer (NuPAGE, Invitrogen Life Technologies); 15 µL of each sample was loaded onto the gels.

For CN-PAGE, purified samples of CHPs were separated by 10%-20% Tris-Glycine Mini Gels (Novex, Invitrogen Life Technologies) at a constant voltage of 140 V for 3.5 hours in running buffer (25 mM Tris-HCl, 192 mM glycine; pH 8.3). Buffer exchange was conducted by spin filtration (Zeba spin desalting columns; Thermo Fisher Scientific) for 100 µL of each protein (1-2 mg/mL) using exchange buffer (20 mM HEPES, 150 mM NaCl, 1 mM $MgCl_2$, 1 mM tris(2-carboxyethyl)phosphine (TCEP); pH 7.2) containing either 10 mM EGTA or 1 mM $CaCl_2$. The protein concentration was determined spectroscopically and each protein sample was diluted with the corresponding buffer to a final concentration of 10 µM. All samples were incubated on ice for 1 hours. Protein sample (20 µl) was mixed with 20 µL 2X native Tris-Glycine sample buffer (Novex Thermo Fisher Scientific) and 40 µL sample was loaded on the gel. Both denaturing and CN-PAGE gels were stained with InstantBlue Protein Stain (Expedeon, Cambridge, UK).

2.4 | Fluorescent probe hydrophobicity (FPH) assay

The protein samples were thawed on ice and buffer exchanged to measuring buffer (20 mM HEPES, 150 mM NaCl, 1 mM $CaCl_2$, 1 mM $MgCl_2$, 1 mM TCEP; pH 7.2) using spin filtration desalting columns (Zeba spin). The protein concentration was determined spectroscopically (NanoDrop 2000). The stock solution of the fluorescent dye, 5000 X SYPRO Orange[26] (Sigma-Aldrich, St. Louis, Missouri, USA), was diluted with the measuring buffer to a final concentration of 12.5 X. For each measurement, 100 µL of 10 µM protein solution and 400 µL 12.5 X dye solution were mixed. This mixture was incubated at 22°C for 5 minutes in the dark. The changes in fluorescence emission of the dye, caused by interaction with hydrophobic regions in CHPs were detected with emission fluorescent spectra from 500 to 700 nm with excitation at 470 nm and a slit width of 10 nm using a fluorescence spectrophotometer (Cary Eclipse, Agilent technologies). For the kinetic experiment, fluorescence was measured at $\lambda_{ex} = 470$ nm and $\lambda_{em} = 585$ nm with a slit width of 10 nm. Measurements were performed with a 500 µl quartz cuvette (High Precision Cell, Hellma GmbH & Co. KG, Müllheim, Germany) at 22°C. 3 µL of 500 mM EGTA (pH 7.2) was added after 3 minutes and 3 µL of 500 mM $CaCl_2$ was added after 8 minutes. For detection of MBP-CBD binding to CHPs, 5 µL of 200 µM MBP-CBD in measuring buffer was added to the cuvette which contained 500 µL of 2 µM CHPs and 10 X dye after 3 minutes of measurement. The fluorescence was measured for another 3 minutes. All measurements were done with three independently produced and purified biological replicates per protein. All data were processed with Origin Pro 2019G (OriginLab Corporation, Northampton, USA).

2.5 | MST for protein-protein interaction

Fluorescence labeling of CHP1 and CHP2 was done according to the manufacture´s protocol with the NHS labeling kit (NanoTemper Technologies GmbH, Munich, Germany). 100 µL of CHP1 or CHP2 protein sample was thawed on ice and buffer exchanged into MST labeling buffer using column A of the kit. CHP1 and CHP2 were diluted with labeling buffer to 40 µM. The fluorescent dye NT647 was dissolved

in MST labeling buffer (final concentration 141 μM) and was mixed with the protein solution in a 1:1 volume ratio. The mixture was incubated for 30 min at room temperature in the dark. The sample was exchanged into measuring buffer (for CHP1: 20 mM HEPES, 150 mM NaCl, 0.05% Tween-20, 10 mM EGTA, 1 mM TCEP; pH 7.5, and for CHP2: 1 mM $CaCl_2$ was used instead of 10 mM EGTA) using column B of the kit. About 180 μL MBP-CBD protein samples were thawed and buffer was exchanged for measuring buffer using spin filtration (PD SpinTrap G-25 column). Protein concentration for CHP1, CHP2, and MBP-CBD and efficiency of labeling were determined as described previously.[24] The extinction coefficient of $\varepsilon_{650} = 250\,000\ M^{-1}cm^{-1}$ was used for the dye NT647. A correction factor of 0.028 was used to correct the additional dye absorption at 280 nm. The labeling efficiency was 30% for CHP1 and 60% for CHP2. Fluorescently labeled CHP1 and CHP2 were diluted with measuring buffer to 20 nM (CHP1) and 10 nM (CHP2). A serial dilution of MBP-CBD was performed as described before.[24] Then,16 dilution steps of MBP-CBD were done for CHP1:MBP-CBD measurements and 13 for CHP2:MBP-CBD measurement covering concentration range from 15 μM to 0.458 nM for CHP1:MBP-CBD and from 300 nM to 0.0366 nM for CHP2:MBP-CBD. After mixing, the samples were incubated for 30 minutes. CHP1:MBP-CBD binding experiment was measured in standard treated capillaries and the CHP2:MBP-CBD was measured in premium coated capillaries (capillaries from NanoTemper Technologies GmbH) at 22°C. All measurements were performed on a Monolith NT.115^{pico} system (NanoTemper Technologies GmbH) using the experimental setup described in Supplemental Table S1. All measurements were done with three independent biological replicates per protein. Five independent titration and measurement series, as technical replicates, was performed per biological replicate. Data were analyzed and graphically processed using MO. Affinity Analysis (NanoTemper Technologies GmbH) and Origin Pro 2019G (OriginLab Corporation).

2.6 | Isothermal titration calorimetry

For ITC measurements, 600 μL aliquots of CHP1, CHP2, and 1 mL aliquots of MBP-CBD for each measurement were thawed on ice and spin concentrated (Vivaspin 500 Centrifugal Concentrators, 10 000 MWCO for CHP1 and CHP2, 30 000 MWCO for MBP-CBD, Sartorius AG, Göttingen, Germany) to a final concentration of 200 μM for CHP1 and CHP2 and 50 μM for MBP-CBD. The concentrated samples were dialyzed in 10 kDa Mini Dialysis Cassettes (Thermo Fisher Scientific) at 4°C for 12 hours in ITC measuring buffer (20 mM HEPES, 150 mM NaCl, 1 mM TCEP; pH 7.5), containing 10 mM EGTA ($-Ca^{2+}$) or 1 mM $CaCl_2$ ($+Ca^{2+}$) and then filtered with 0.2 μm centrifugal filters (VWR international, Pennsylvania, USA). All protein samples were diluted to the final concentration with the dialysis buffer. The final concentrations of all samples were determined spectroscopically.

All ITC measurements were carried out on a MicroCal VP-ITC instrument (Malvern Instruments, Worcestershire, UK) at 22°C with a constant stirring speed of 394 rpm. Samples were degassed prior to loading into the calorimeter. Biological triplicates were measured. For CHP1:MBP-CBD interaction, the cell was filled with 1.4 mL of 3 μM MBP-CBD, and 300 μL of 30 μM CHP1 was loaded into the syringe. For CHP2: MBP-CBD interaction, the cell was filled with 1.4 mL of 2 μM MBP-CBD and 300 μL of 20 μM CHP2 was loaded into the syringe. Typically, 10 μL injections were made every 8 minutes for CHP1:MBP-CBD and every 7 minutes for CHP2:MBP-CBD. The heat of an initial injection of 1 μL was excluded from the analysis to eliminate its higher error. All blank experiments were performed by titrating CHP1 and CHP2 into measuring buffers. MicroCal PEAQ-ITC analysis software (Malvern Instruments) was used for data evaluation. Fitting of ITC data was performed with a triple-shift approach as described in detail by Fuchs et al.[24]

3 | RESULTS

3.1 | Gel shift assay under native conditions proves Ca^{2+} binding to purified recombinant CHP1 and CHP2

In order to characterize the isoform-specific properties of human CHP1 and CHP2, the studies were performed with CHPs devoid of affinity tags. These tags could fold back in the hydrophobic binding pocket of CHPs as seen in the X-ray structure of rat CHP1.[1,27] Human CHP1 and CHP2, as well as CHP3 for comparison, were produced by heterologous expression and individual purification strategies were devised. His-tagged CHP1 and CHP2 were subjected to TEV-protease cleavage after IMAC purification to remove the amino-terminal affinity-tag. CHP2 was additionally purified by HIC. Wild-type CHP3 was purified by HIC. After size exclusion chromatography as common final purification step, isoforms were obtained at high purity and homogeneity as judged by SDS-PAGE analysis (Figure 1A) and analytical size exclusion chromatography (Supplemental Figure S1). To unambiguously probe Ca^{2+}-binding to CHPs and to prove the functionality of the purified proteins, we utilized CN-PAGE (Figure 1B). In that gel system, differences in the mobility of the three CHPs should depend mainly on their charge, as CHPs have similar molecular masses between 23 and 25 kDa but should have different surface charges as their isoelectric points are different (Table 1 and Figure 1B). Indeed, the highest mobility was observed for CHP3, which has a calculated charge of −16.6. CHP1 showed medium

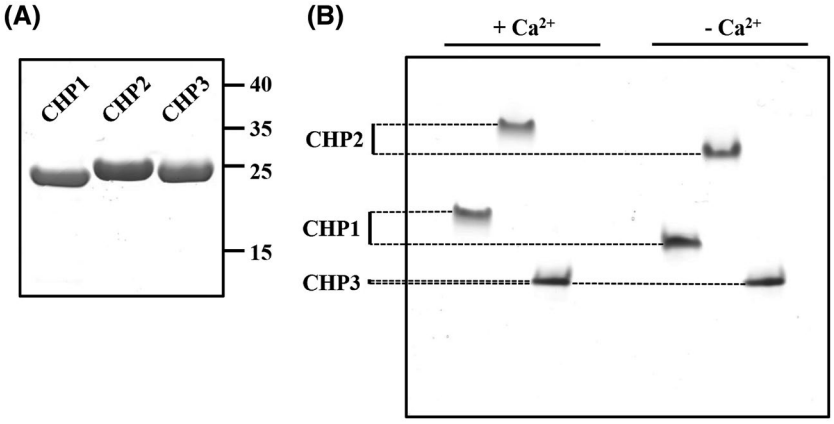

FIGURE 1 Purified CHP1, CHP2, and CHP3 at denaturing conditions (A) and Ca^{2+} effect on electrophoretic mobility at native conditions (B). A, Coomassie-stained gel after SDS-PAGE separation of 3.5 μg protein per lane. The molecular mass of co-separated standard proteins is given in kDa. B, CHP1, CHP2, and CHP3 were preincubated in buffer containing 1 mM $CaCl_2$ ($+Ca^{2+}$) or 10 mM EGTA ($-Ca^{2+}$). Coomassie-stained gel after CN-PAGE separation of 4.5 μg protein per lane

TABLE 1 Properties of CHP isoforms

Isoform	UniProt ID	Number of functional EF-hands (#)	Molecular mass (kDa)	Calculated pI	Calculated charge at pH 8.3	
					$+Ca^{2+}$	$-Ca^{2+}$
CHP1	Q99653	2	22.5	5.1	−6.9	−10.9
CHP2	O43745	2	22.5	6.3	−0.8	−4.8
CHP3	Q96BS2	1	24.7	4.9	−14.6	−16.6

Note: The molecular mass was calculated with ProtParam (ExPASy); pI and charge were calculated with ProteinCalculator v3.4 (http://protcalc.sourceforge.net/).

mobility corresponding to the calculated charge of −10.9. Slowest mobility was seen for CHP2, which has a calculated charge of −4.8. Notably, addition of Ca^{2+} decreased the electrophoretic mobility of CHPs, indicating lowered charge and thus Ca^{2+}-binding to their functional EF-hands. Changes were substantial for CHP1 and CHP2, which both have two functional EF-hands, and they are little for CHP3, which has a single functional EF-hand (Figure 1B). As Ca^{2+}-binding to EFCaBPs in general results in changes of protein conformation,[28] a change in Stokes radius is likely to contribute to the observed gel shifts. The contribution of charge compensation and conformational change cannot be distinguished in gel shift assays, but conformational changes can be probed with fluorescence methods.

3.2 | Monitoring Ca^{2+}-induced conformational changes of CHPs using the FPH assay

Ca^{2+}-induced conformational changes observed in EFCaBPs typically result in the opening of their hydrophobic pocket.[28] We therefore used a hydrophobic fluorescent probe (SYPRO Orange) to directly monitor whether CHPs undergo such conformational changes. The dye´s fluorescence is quenched by aqueous solvents, but strongly increases in hydrophobic environment for instance upon its binding to hydrophobic protein surfaces.[26] So far it has been used in differential scanning fluorimetry to determine the thermal stability of proteins, as unfolding of proteins results in exposure of hydrophobic protein parts.[26] In the fluorescence probe hydrophobicity (FPH) assay, purified CHPs were preincubated with the probe and fluorescence spectra were recorded in the presence and absence of Ca^{2+}. In all CHPs, fluorescence emission at 585 nm was observed, indicating binding of the probe to the native protein (Figure 2A). Fluorescence emission and binding of the probe were also detected for the classical EF-hand protein CaM used as a positive control. Fluorescence intensity of a fusion protein of MBP linked to CBD, the CHP-binding part of NHE1[24] used as a negative control was negligible, indicating that the dye did not bind to MBP-CBD. Also, a buffer control was without fluorescent signal. Interestingly, fluorescence intensity varied between the isoforms. In the presence of Ca^{2+}, CHP2 and CHP3 showed similar fluorescence intensity and for CHP1, it was about half compared to the other CHPs. Furthermore, Ca^{2+}-depletion resulted in isoform-specific fluorescence changes. Ca^{2+}-depletion substantially decreased fluorescence by ~50% for CHP2 and moderately by ~25% for CHP3, whereas fluorescence increased by ~100% for CHP1. For CaM, Ca^{2+}-depletion resulted in a ~80%

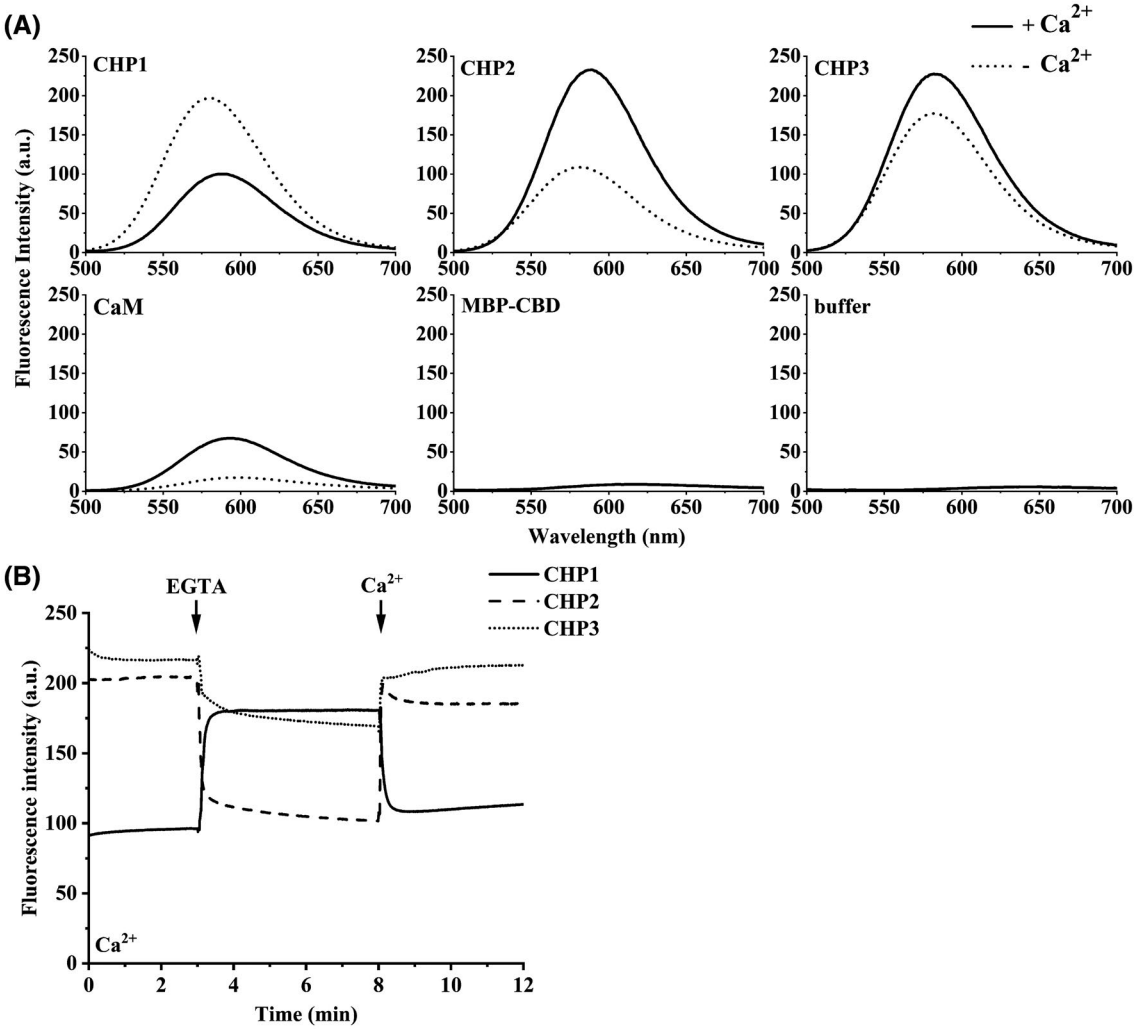

FIGURE 2 Ca^{2+}-induced conformational changes of CHP1, CHP2, CHP3, and CaM analyzed with FPH assay. A, Fluorescence emission spectra (500-700 nm; $\lambda_{ex} = 470$ nm) of CHPs and CaM incubated with the hydrophobic fluorescent probe in the presence or absence of 1 mM Ca^{2+}. As negative controls, the same experiment was performed with MBP-CBD and in the absence of protein (buffer). B, Kinetic fluorescence assay probing the reversibility of Ca^{2+}-induced conformational changes of CHPs. Proteins were preincubated with dye in the presence of 1 mM $CaCl_2$ (indicated in the left bottom corner). Ca^{2+} depletion by EGTA addition at a final concentration of 3 mM is indicated with an arrow. Re-supplementation of Ca^{2+} by addition of $CaCl_2$ to a final concentration of 4 mM is indicated with the arrow at 8 minutes. The fluorescence of the dye was monitored at $\lambda_{ex} = 470$ nm and $\lambda_{em} = 585$ nm at 22°C

decrease of fluorescence intensity. Ca^{2+}-free CaM adopts a closed conformation, in which the hydrophobic patches important for target protein binding are less solvent exposed.[29] Correspondingly, low fluorescence intensity was noted for CaM in the absence of Ca^{2+}. Taken together, the FPH assay is well suited to monitor conformational changes (Figure 2A).

The results indicate Ca^{2+}-induced conformational changes in CHPs. To exclude that the fluorescence arises from binding of the dye to unfolded protein parts, reversibility of the fluorescence was monitored over time (Figure 2B, Supplemental Figure S2). The reaction was started with CHPs in presence of Ca^{2+}. Upon Ca^{2+}-depletion by addition of EGTA, fluorescence intensity decreased for CHP2 and CHP3 and increased for CHP1 as expected from experiments described above (Figure 2). Subsequent supplementation with Ca^{2+} reversed the fluorescent changes. All reactions were rapid, though isoform-specific differences in kinetics were visible that will be addressed in future studies. As the interaction of the probe to hydrophobic parts of CHPs was reversible, one can safely conclude that the Ca^{2+}-induced changes in fluorescence reflect a conformational change of CHPs. The dye most likely binds to the hydrophobic pocket of CHPs, the binding site for CBD of NHE1.

3.3 | CBD binding to CHPs reduces their hydrophobicity and competes with the fluorescent probe

According to X-ray and nuclear magnetic resonance spectroscopy (NMR) structures of CHP1 and CHP2 in complex

with the CBD fragment of NHE1, CBD forms in the bound state an amphipathic helix that occupies the hydrophobic binding pocket nearly completely.[5,30] CBD should thus replace bound fluorescent probes which would lead to fluorescence decrease in competition experiments. MBP-CBD was previously used for characterization of the binding of CHP3 to NHE1.[24] After preincubation of CHPs with the fluorescent probe, addition of MBP-CBD led to an immediate decrease of fluorescence intensity (Figure 3, Supplemental Figure S3). Effects were similar in the presence and absence of Ca^{2+}. Thus, CBD binding decreased the overall hydrophobicity of CHPs. As a negative control, MPB-CBD_{con} was used, a fusion protein in which side chain substitutions disable the binding interaction.[24] Fluorescence intensities remained stable after addition of MPB-CBD_{con} (Supplemental Figure S4), emphasizing the specific binding of CBD to CHPs. The fluorescence was not completely quenched upon CBD binding to all CHPs. This indicates incomplete replacement of the probe by CBD or additional hydrophobic patches involved in probe binding (Figure 3). Taken together, we proved that the probe binds to the hydrophobic pocket and can be replaced by CBD, and the FPH assay can be used to monitor target binding of CHPs.

3.4 | Ca^{2+}-depletion reduces the high affinity binding of CHP2 to NHE1 but not of CHP1 to NHE1

Next, we asked whether Ca^{2+} affects the binding interaction of CHP1 and CHP2 with NHE1. Quantitative characterization of the CHP1 and CHP2 interaction with CBD was first performed by MST. The optimized experimental conditions were then used for the thermodynamic characterization by ITC as recently described.[24] Three biological replicates with data points averaged for five technical replicates were measured for Ca^{2+}-free CHP1 and Ca^{2+}-bound CHP2 (Figure 4). The T-jump analysis was chosen for the calculation of the binding isotherms.[31] Both, CHP1 and CHP2 bound to CBD with nanomolar affinities (K_D (CHP1:CBD) = 59.5 ± 1.1 nM and K_D (CHP2:CBD) = 3.3 ± 0.5 nM) (Figure 4, Supplemental Figure S5, Supplemental Table S2). For comparison, a K_D of 56 nM was determined by MST for the interaction of CHP3:CBD.[24] The ITC measurements were performed in the presence and absence of Ca^{2+} with three independently produced and purified biological samples per protein (Figure 5). The triple-shift procedure was applied to correct for the concentration of active CHP1, CHP2, and CBD (Supplemental Tables S3-S6) as described in the previous study.[24] Subsequently, global nonlinear regression of the data points using an one set of sites model[32] was performed and the confidence of the fit was calculated with error support plane analysis (Supplemental Figures S6-S9 and Supplemental Tables S3-S6).[24,33]

The CHP1:CBD interaction was exothermic both in the presence and absence of Ca^{2+}. Notably, the enthalpy contribution was smaller in the presence of Ca^{2+} ($\Delta H = -119$ kJ/mol) than in its absence ($\Delta H = -148$ kJ/mol) (Figure 5C). The enthalpy difference in the two conditions was compensated by a positive entropy contribution, which was smaller in the presence of Ca^{2+} ($-T\Delta S° = 73$ kJ/mol), than in its absence ($-T\Delta S° = 102$ kJ/mol) (Figure 5C). This resulted in the same free enthalpy of binding in both conditions ($-Ca^{2+}$: $\Delta G° = -45.7$ kJ/mol; $+Ca^{2+}$: $\Delta G° = -45.8$ kJ/mol) (Figure 5C). As the differences in K_D values obtained were very small ($-Ca^{2+}$: 8.1 nM; $+Ca^{2+}$: 7.7 nM; Table 2), one can conclude that the affinities of the CHP1:CBD interaction are unaffected by Ca^{2+} (Figure 5C).

The CHP2:CBD interaction is also exothermic with lower enthalpic contribution in the presence of Ca^{2+} ($+Ca^{2+}$: ΔH = -94.1 kJ/mol) than in the absence ($-Ca^{2+}$: $\Delta H = -147$ kJ/mol) (Figure 5F). The positive entropic contribution was substantially lower in comparison to the CHP1:CBD interaction

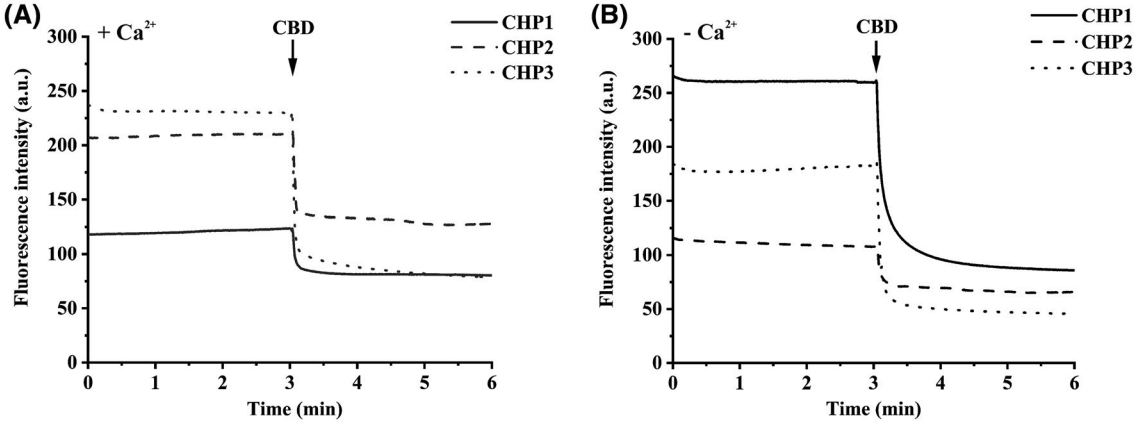

FIGURE 3 CBD binding to CHPs quenched the fluorescence of the probe in the presence (A), and absence of Ca^{2+} (B). CHPs (2 μM) were preincubated with dye (final concentration 10×) at 22°C. Then, equimolar amount of MBP-CBD was added (indicated with arrow). The fluorescence of the dye was monitored as described in Figure 2B

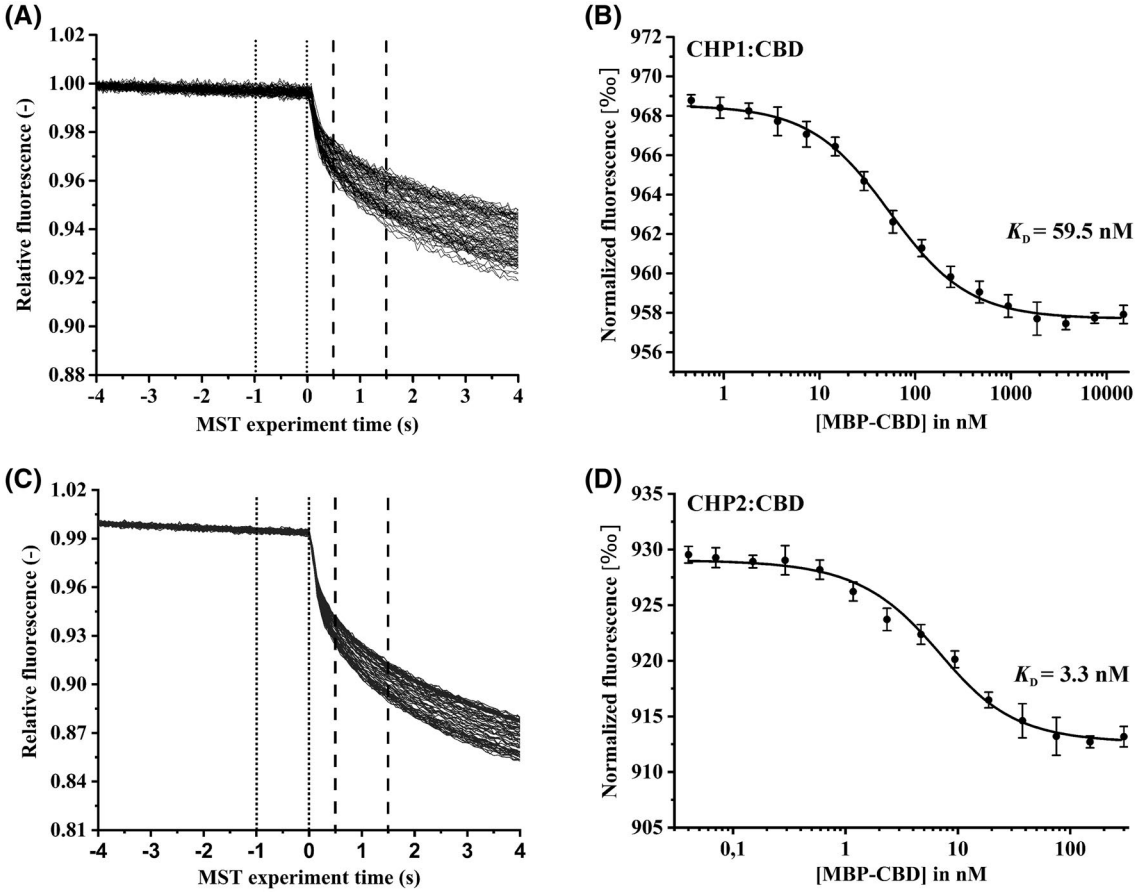

FIGURE 4 Interaction of CHP1 and CHP2 with CBD analyzed with microscale thermophoresis. Thermophoresis time traces of CHP1:CBD (A) and CHP2:CBD interaction (C) from five independent titration series of one biological replicate, all normalized to a starting value of 1. Time spans for F_{cold} and F_{hot} are represented with dotted and dashed lines. Complete time traces are shown in Supplemental Fig. S5. The resulting binding curves for CHP1:CBD (B) and CHP2:CBD (D) are derived from (A) and (C), with each dot indicating the average of F_{norm}, and error bars showing the standard deviation. The solid line represents the best fit of the data using the bimolecular binding model. Data summary of biological triplicates is shown in supplemental Table S2. A mean $K_D = 59.5 \pm 1.1$ nM was obtained for the CHP1:CBD interaction, and $K_D = 3.3 \pm 0.5$ nM was obtained for the CHP2:CBD interaction

in the presence of Ca^{2+} ($-T\Delta S° = 46$ kJ/mol), whereas it was similar in the absence of Ca^{2+} ($-T\Delta S° = 104$ kJ/mol) (Figure 5F). Overall, these contributions resulted in a small difference of the $\Delta G°$ between the two conditions ($+Ca^{2+}$: $\Delta G° = -48.1$ kJ/mol; $-Ca^{2+}$: $\Delta G° = -43.2$ kJ/mol). The dissociation constant was substantially lower in the presence of Ca^{2+}, than in the absence ($+Ca^{2+}$: 3.2 nM; $-Ca^{2+}$: 22 nM; Table 2). That indicates an increased affinity of the Ca^{2+}-bound CHP2 to CBD (Figure 5F).

In summary, the enthalpic and entropic contributions to the CHP1:CBD interaction are larger than those for CHP2:CBD in the presence of Ca^{2+}. For both proteins, however, the exothermic interaction is associated with a positive entropic contribution, so that the free enthalpy does not differ so much. It is noteworthy, that the Ca^{2+} effect on the interaction is isoform specific. The affinity of the CHP2:CBD interaction decreases in the absence of Ca^{2+}, whereas the affinity of the CHP1:CBD interaction is not affected by lack of Ca^{2+}.

4 | DISCUSSION

Calcineurin B homologous proteins belong to the EFCaBP family and are involved in regulatory pathways.[1] Notably, they are essential for trafficking and activity of the sodium/proton exchangers which control intracellular pH.[13] CHP1 and CHP2 share high sequence and structure homology. However, CHP1 is ubiquitously expressed, whereas CHP2 is mainly abundant in fast-proliferating cells.[1] CHP1 and CHP2 bind Ca^{2+} with high affinity.[6,7] In this study, we developed an assay to detect Ca^{2+}-induced conformational changes of EFCaBPs with focus on CHPs. Further, we directly compared the properties of CHPs and the effect of Ca^{2+} on CHPs:NHE1 interaction using a recently established system.[24]

For high quality biochemical and biophysical characterization, we produced and purified human CHP1 and CHP2. Highly pure recombinant CHP1 and CHP2 protein samples were reproducibly obtained providing the basis for

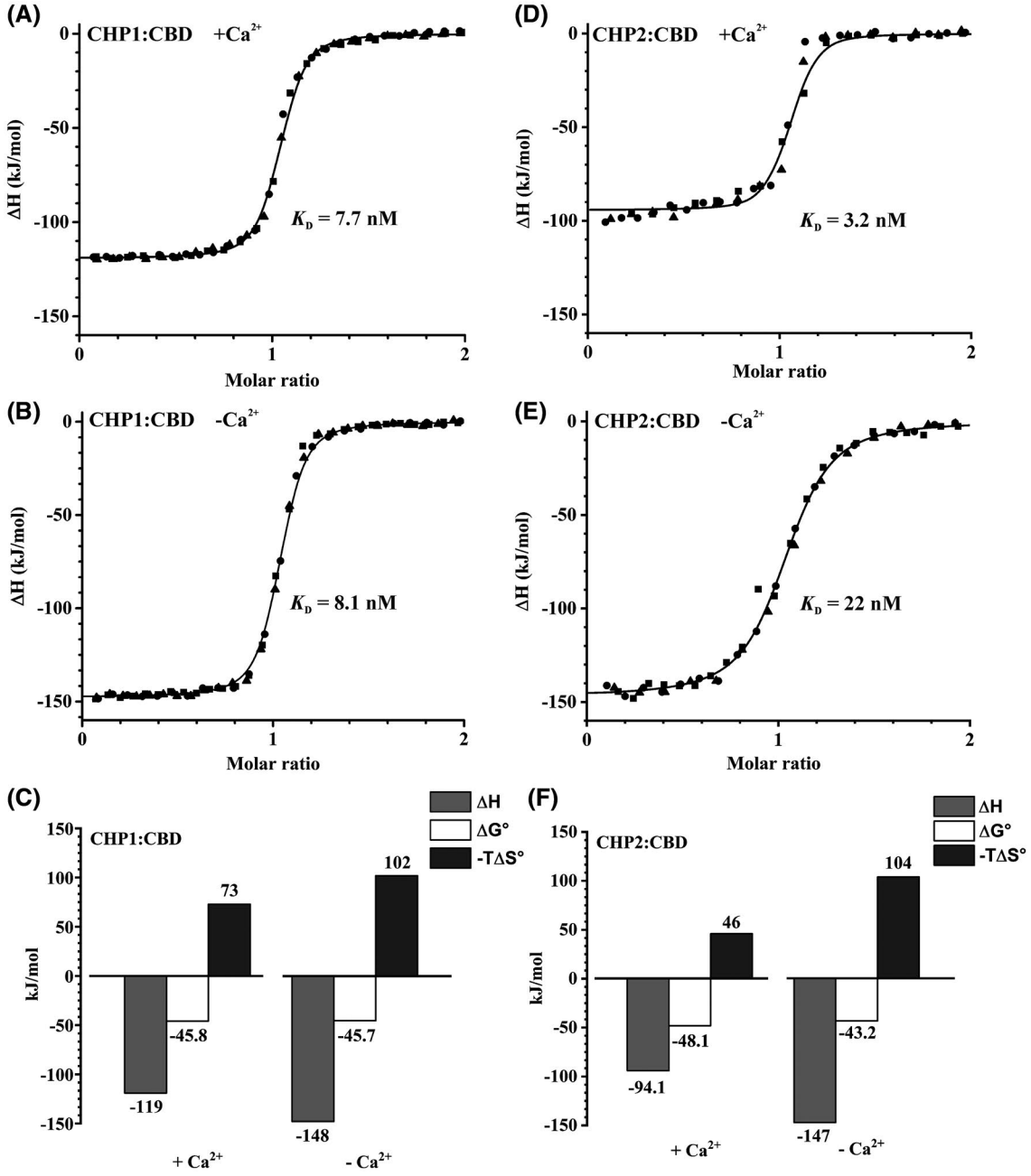

FIGURE 5 Interaction of CHP1 and CHP2 with CBD analyzed by ITC in the presence and absence of Ca^{2+}. ITC data were obtained by titrating CHP1 into CBD in the presence (A) and absence of Ca^{2+} (B) or by titrating CHP2 into CBD in the presence (D) and absence of Ca^{2+} (E). Data are shown as a function of [CHP1]/[MBP-CBD] or [CHP2]/[MBP-CBD] in molar ratio. Squares, triangles, and dots each indicate a biological replicate. The curves of biological triplicates were subjected to a triple-shift correction assuming n = 1. Individual active concentrations of [CHP1] and [MBP-CBD] or [CHP2] and [MBP-CBD] are shown in supplemental Tables S3-S6. The solid lines represent the global fits. All measurements were performed at 22°C. All thermodynamic parameters are summarized as column diagrams for the CHP1:CBD interaction (C) and the CHP2:CBD interaction (F)

characterization of Ca^{2+}-induced conformational changes and quantitative in vitro binding analysis. Previous studies used either partially purified His-tagged CHPs or the CHP:CBD complex to estimate Ca^{2+} binding affinities[6,7] and for structure determination.[5,27,30] In a CBD-free structure of CHP1, the C-terminal His-tag and additional linker region together with the αJ-helix blocked the hydrophobic pocket of CHP1, which is the target binding site.[27] The C-terminal tag might have stabilized the structure of CHP1. This is beneficial for crystallization, but could artificially affect in vitro binding analysis. As CHP1 and CHP2 are rather small proteins, an addition of an N-terminal affinity tag might also influence in vitro binding assays.[34] Thus, we inserted a TEV cleavage site after the N-terminal His_6-tag and performed cleavage during

TABLE 2 Thermodynamic parameters of the interaction between CHP1 and CBD and between CHP2 and CBD obtained by ITC

Interaction	K_D (nM)	ΔH (kJ/mol)	ΔG° (kJ/mol)	−TΔS° (kJ/mol)
$+Ca^{2+}$ CHP1:CBD	7.7 [6.8, 8.7]	−119	−45.8 [−46.1, −45.5]	73 [72, 74]
$-Ca^{2+}$ CHP1:CBD	8.1 [7.4, 8.8]	−148	−45.7 [−45.9, −45.5]	102 [102, 103]
$+Ca^{2+}$ CHP2:CBD	3.2 [2.1, 4.6]	−94.1	−48.1 [−49.0, −47.1]	46 [45, 47]
$-Ca^{2+}$ CHP2:CBD	22 [19, 25]	−147	−43.2 [−43.6, −42.9]	104 [103, 105]

Note: The confidence intervals for NSSD <1.1 are shown in square brackets (see Supplemental Tables S3–S6 and comments there for details). Confidence intervals for ΔG° and −TΔS° were calculated from the confidence intervals of K_D.

purification. Two additional amino acids (Gly-Ala) remained after cleavage with potentially negligible effects. We reproducibly obtained sufficient amounts of proteins for quantitative in vitro studies.

We observed substantially reduced mobility of Ca^{2+}-bound CHP1 and CHP2 in CN-PAGE. So far, Barroso *et* al. reported a small Ca^{2+}-dependent decrease of rat CHP1 mobility in CN-PAGE gels.[12] 10%-20% polyacrylamide gradient gels are more suitable for separation of small proteins, like CaM.[35] We improved the readout of CN-PAGE for the detection of Ca^{2+}-dependency with high percent gradient gels. CHP3 undergoes a Ca^{2+}-induced conformational change,[14] but despite the high resolution gels, the mobility shift was little. This may be due to the fact that CHP3 has only one functional EF-hand.[14]

The mobility shift of CHPs in CN-PAGE can be caused by a conformational change and/or by the additional charge upon Ca^{2+} binding.[36] For unambiguous detection of Ca^{2+}-induced conformational changes of CHP1, CHP2, and CHP3, we used a hydrophobic fluorescent probe. The fluorescence of this dye is quenched in hydrophilic and enhanced in hydrophobic environment.[37] 8-Anilinonaphthalene-1-sulfonic acid (ANS) and its derivatives are widely used to detect Ca^{2+}-induced conformational changes of EFCaBPs.[38] Yet, ANS binds to proteins not only by hydrophobic but also by electrostatic interactions.[39,40] Therefore, we used SYPRO® Orange to detect Ca^{2+}-induced hydrophobicity changes. This dye is typically used to analyze protein stability in thermal shift assays.[41] In comparison to ANS, it has two long aliphatic chains and the net charge is neutral.[37] Thus, the dye is more elongated and interacts specifically with hydrophobic regions.[37] It should be in general advantageous to detect the Ca^{2+}-dependent accessibility of EFCaBPs' hydrophobic pockets. As a proof-of-principle, we showed enhanced fluorescence and thus binding of the dye to the hydrophobic patches of CaM, which become exposed in the presence of Ca^{2+}.

With this FPH assay, we detected enhanced fluorescence in the presence of Ca^{2+} for CHP2 and CHP3 similar to CaM. This is in line with a Ca^{2+}-induced conformational change that makes a hydrophobic pocket of these CHPs more accessible for the dye. For CHP3, these data corroborate previous results, in which a Ca^{2+}-induced conformational change was shown by intrinsic tryptophan fluorescence measurements and circular dichroism spectroscopy.[14] For CHP2, such experiments for wild-type protein were lacking. The data obtained with the FPH assay in the present study documented a Ca^{2+}-induced conformational change of CHP2 that can be reversed by depletion of Ca^{2+}. Notably, the Ca^{2+}-induced hydrophobicity increase was substantially higher for CHP2 than for CHP3 (Figure 2). Upon Ca^{2+}-depletion, residual dye remained bound to CHPs indicating accessibility of the hydrophobic pocket both in the presence and absence of Ca^{2+}. In contrast to CHP2 and CHP3, we detected a fluorescence intensity decrease for CHP1 in the presence of Ca^{2+} with the FPH assay (Figure 2A). This may reflect that the hydrophobic pocket of CHP1 is more occluded in Ca^{2+}-free state increasing its hydrophobicity (Figure 6A). Taken together, all of the CHPs respond to Ca^{2+} with a conformational change that can be reversed by Ca^{2+}-depletion. Yet, the nature of the response is isoform specific. The FPH assay was also applied to probe the binding of CHPs to CBD. A decrease of fluorescence after CBD binding indicated that the dye binds in the hydrophobic pocket in a similar manner for the CHP isoforms.

As mentioned above, CHP1 and CHP2 act as important regulatory proteins for Na^+/H^+ exchangers including NHE1.[1] We performed ITC measurements to compare the thermodynamic parameters and the Ca^{2+}-dependency of these interactions. Both CHPs bound to CBD with nanomolar affinities (Table 2), very similar to that reported for CHP3.[24] Whereas Ca^{2+} did not affect the binding affinity of CHP1 (Figure 6A), the K_D for the CHP2:CBD interaction increased 7-fold when Ca^{2+} was absent (Figure 6B). This is in line with co-immunoprecipitation experiments which reported reduced CHP2:CBD interaction upon Ca^{2+}-depletion.[7] The effect of Ca^{2+} on the CHP2:CBD interaction can be interpreted in the light of the data from the FPH assay. The hydrophobicity of CHP2 was clearly reduced upon Ca^{2+}-depletion (Figure 2) indicating lower accessibility of the hydrophobic pocket (Figure 6B). Thus, the pocket has to open for binding of the amphipathic CBD helix. We propose an additional rate limiting step for the binding reaction at Ca^{2+}-free condition. Kinetic studies are required to address this question.

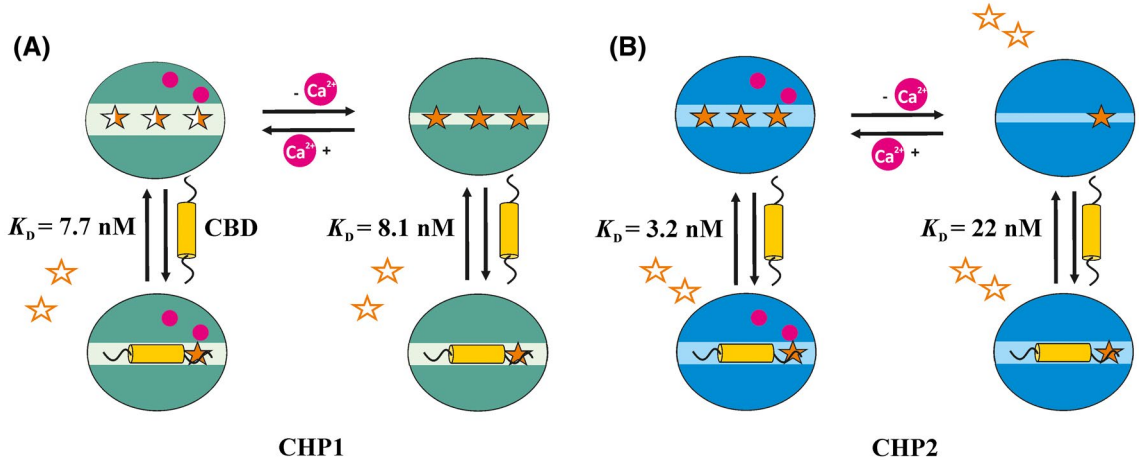

FIGURE 6 Schematic presentation of Ca^{2+} effect on conformation of CHP1 and CHP2 and their interaction with CBD. A, The fluorescent probe binds to the hydrophobic pocket of CHP1 in the presence and absence of Ca^{2+}. However, Ca^{2+} release leads only to partial "closing" of the CHP1 hydrophobic pocket. The pocket remains accessible to the dye and CBD. In this case Ca^{2+} does not affect the CHP1:CBD binding affinity. B, The hydrophobic pocket of CHP2 is accessible for the fluorescent probe in the presence of Ca^{2+}. The release of Ca^{2+} results in the "closing" of the hydrophobic pocket and decreased accessibility for the dye and CBD. This also affects interaction of CHP2:CBD, resulting in the increase of K_D from 3.2 nM (in the presence of Ca^{2+}) to 22 nM (in the absence of Ca^{2+}). In both cases, binding of CBD to CHPs results in the release of the hydrophobic fluorescent probe

The thermodynamic parameters show that the CHP1 and CHP2 interaction with NHE1 is exothermic, more enthalpy driven and overcomes an entropy penalty, as it was described for CHP3.[24] Noteworthy, the $\Delta G°$ values for the interactions are very similar (−40 to −49 kJ/mol) for all CHPs, despite the substantial variations in entropy and enthalpy among the individual CHP isoforms. The enthalpy-entropy compensation[42] holds true for all CHPs. We suggested that the enthalpic contribution derives from the transition of the disordered structure of CBD in unbound state to the amphipathic helix in bound state.[24] Values of −2.9 kJ/mol were described per residue folding into a helix.[43] The enthalpic contribution of the helix formation should be similar for the CHP isoforms. The notable range in ΔH for the different isoforms (−148 to −94 kJ/mol) is likely to derive from their different individual properties, as reflected for instance in their individual profiles for Ca^{2+}-induced conformational changes. Furthermore, the high $-T\Delta S°$ for the CHP1:CBD interaction as compared to CHP2 in the presence of Ca^{2+} is striking. It may derive from higher inherent mobility of CHP1. Without target peptides, the protein was reported to tend to aggregate.[5,6] Yet, the interaction of CHP1 and CHP2 with CBD has a consistently lower $-T\Delta S°$ of 30-50 kJ/mol in the presence of Ca^{2+} as compared to the Ca^{2+} -free state. This can be explained by more water molecules being replaced by CBD from a more ordered network in the open hydrophobic pocket. The exposure of hydrocarbons to water at room temperature has a suggested contribution of about $-T\Delta S° = 3$ kJ/mol per methylene group.[44] Furthermore, binding of Ca^{2+} to CHPs most likely reduces their flexibility thus lowering the entropic penalty. Further studies such as molecular dynamics simulations or an NMR structure of Ca^{2+}-unbound and -bound states can improve our understanding how Ca^{2+}-binding affects the structure and regulates specifically different CHP isoforms.

In conclusion, the novel FPH assay can be generally applied for characterization of EFCaBPs, which typically open a hydrophobic pocket to bind their target.[45] CHP1 and CHP2 both undergo a Ca^{2+}-induced conformational change, providing the structural basis for Ca^{2+}-triggered regulatory activity on target proteins. CHP1 binds with high affinity to NHE1 irrespective of presence or absence of Ca^{2+}, whereas the interaction of CHP2 with NHE1 is directly modulated, namely strongly enhanced by Ca^{2+}. Thus, Ca^{2+} might have a direct effect on CHP2 function in the cell, whereas CHP1:NHE1 interaction might be regulated by Ca^{2+} only when it is myristoylated. A Ca^{2+}-mediated myristoyl switch was reported for N-myristoylated CHP1.[12,46,47] Our data enhance the detailed understanding of the molecular mechanisms that underlie the regulatory interactions with NHE1, which are critical for control of intracellular ion homeostasis and cell volume. Future studies have to compare kinetic properties and as well as the impact of myristoylation on the regulatory interaction between CHP isoforms and NHE1.

ACKNOWLEDGMENTS

This work was supported by the Deutsche Forschungsgemeinschaft (DFG, German Research Foundation) – SFB 746, Project-ID 403222702 / SFB 1381 to C.H., Project-ID 278002225 / RTG 2202 to C.H. and H.H.), and by the DFG under Germany´s Excellence Initiative (BIOSS – EXC-294) to C.H. and H.H. Gefördert durch die Deutsche Forschungsgemeinschaft (DFG) im Rahmen der

Exzellenzstrategie des Bundes und der Länder – EXC-2189 – Projektnummer 390939984 (funded by the DFG under Germany´s Excellence Strategy – EXC-2189 – Project ID: 390939984 to C.H. and H.H.). We thank Dr. Arie Geerlof (EMBL) for kindly providing the vector pBADM-11.

CONFLICT OF INTEREST

The authors declare no conflict of interest.

AUTHOR CONTRIBUTIONS

S. Liang, S. Fuchs, E.V. Mymrikov, C. Hunte conceived the study; S. Liang, S. Fuchs prepared the proteins. S. Liang performed PAGE, MST, and fluorescence experiments; S. Liang, S. Fuchs, E.V. Mymrikov, C. Hunte analyzed the data. H. Heerklotz, A. Stulz, M. Kaiser, S. Liang performed, and evaluated the ITC experiments; all authors discussed the results and contributed to writing of the manuscript.

REFERENCES

1. Di Sole F, Vadnagara K, Moe OW, Babich V. Calcineurin homologous protein: a multifunctional Ca2+-binding protein family. *Am J Physiol Renal Physiol*. 2012;303:F165-F179.
2. *The human protein atlas*. https://www.proteinatlas.org/
3. Pang T, Wakabayashi S, Shigekawa M. Expression of calcineurin B homologous protein 2 protects serum deprivation-induced cell death by serum-independent activation of Na+/H+ exchanger. *J Biol Chem*. 2002;277:43771-43777.
4. Ben Ammar Y, Takeda S, Sugawara M, Miyano M, Mori H, Wakabayashi S. Crystallization and preliminary crystallographic analysis of the human calcineurin homologous protein CHP2 bound to the cytoplasmic region of the Na+/H+ exchanger NHE1. *Acta Crystallogr Sect F Struct Biol Cryst Commun*. 2005;61:956-958.
5. Mishima M, Wakabayashi S, Kojima C. Solution structure of the cytoplasmic region of Na+/H+ exchanger 1 complexed with essential cofactor calcineurin B homologous protein 1. *J Biol Chem*. 2007;282:2741-2751.
6. Pang T, Hisamitsu T, Mori H, Shigekawa M, Wakabayashi S. Role of calcineurin B homologous protein in pH regulation by the Na+/H+ exchanger 1: tightly bound Ca2+ ions as important structural elements. *Biochemistry*. 2004;43:3628-3636.
7. Li QH, Wang LH, Lin YN, et al. Nuclear accumulation of calcineurin B homologous protein 2 (CHP2) results in enhanced proliferation of tumor cells. *Genes Cells*. 2011;16:416-426.
8. Chazin WJ. Relating form and function of EF-Hand calcium binding proteins. *Acc Chem Res*. 2011;44:171-179.
9. Grabarek Z. Structural basis for diversity of the EF-hand calcium-binding proteins. *J Mol Biol*. 2006;359:509-525.
10. Nelson MR, Chazin WJ. Structures of EF-hand Ca(2+)-binding proteins: diversity in the organization, packing and response to Ca2+ binding. *Biometals*. 1998;11:297-318.
11. Finn BE, Evenas J, Drakenberg T, Waltho JP, Thulin E, Forsen S. Calcium-induced structural changes and domain autonomy in calmodulin. *Nat Struct Biol*. 1995;2:777-783.
12. Barroso MR, Bernd KK, DeWitt ND, Chang A, Mills K, Sztul ES. A novel Ca-binding protein, p22, is required for constitutive membrane traffic. *J Biol Chem*. 1996;271:10183-10187.
13. Pang TX, Su XH, Wakabayashi S, Shigekawa R. Calcineurin homologous protein as an essential cofactor for Na+/H+ exchangers. *J Biol Chem*. 2001;276:17367-17372.
14. Gutierrez-Ford C, Levay K, Gomes AV, et al. Characterization of tescalcin, a novel EF-hand protein with a single Ca2+-binding site: metal-binding properties, localization in tissues and cells, and effect on calcineurin. *Biochemistry*. 2003;42:14553-14565.
15. Nakamura N, Miyake Y, Matsushita M, Tanaka S, Inoue H, Kanazawa H. KIF1Bβ2, capable of interacting with CHP, is localized to synaptic vesicles. *J Biochem*. 2002;132:483-491.
16. Kuwahara H, Kamei J, Nakamura N, Matsumoto M, Inoue H, Kanazawa H. The apoptosis-inducing protein kinase DRAK2 is inhibited in a calcium-dependent manner by the calcium-binding protein CHP. *J Biochem*. 2003;134:245-250.
17. Li GD, Zhang X, Li R, et al. CHP2 activates the calcineurin/nuclear factor of activated T cells signaling pathway and enhances the oncogenic potential of HEK293 cells. *J Biol Chem*. 2008;283:32660-32668.
18. Donowitz M, Ming Tse C, Fuster D. SLC9/NHE gene family, a plasma membrane and organellar family of Na(+)/H(+) exchangers. *Mol Aspects Med*. 2013;34:236-251.
19. Mailander J, Muller-Esterl W, Dedio J. Human homolog of mouse tescalcin associates with Na(+)/H(+) exchanger type-1. *FEBS Lett*. 2001;507:331-335.
20. Liu Y, Zaun HC, Orlowski J, Ackerman SL. CHP1-mediated NHE1 biosynthetic maturation is required for Purkinje cell axon homeostasis. *J Neurosci*. 2013;33:12656-12669.
21. Mendoza-Ferreira N, Coutelier M, Janzen E, et al. Biallelic CHP1 mutation causes human autosomal recessive ataxia by impairing NHE1 function. *Neurol Genet*. 2018;4:e209.
22. Guissart C, Li X, Leheup B, et al. Mutation of SLC9A1, encoding the major Na(+)/H(+) exchanger, causes ataxia-deafness Lichtenstein-Knorr syndrome. *Hum Mol Genet*. 2015;24:463-470.
23. Iwama K, Osaka H, Ikeda T, et al. A novel SLC9A1 mutation causes cerebellar ataxia. *J Hum Genet*. 2018;63:1049-1054.
24. Fuchs S, Hansen SC, Markones M, Mymrikov EV, Heerklotz H, Hunte C. Calcineurin B homologous protein 3 binds with high affinity to the CHP binding domain of the human sodium/proton exchanger NHE1. *Sci Rep*. 2018;8:14837.
25. Battey NH, Venis MA. Calcium-dependent hydrophobic interaction chromatography. *Methods Mol Biol*. 1992;11:73-80.
26. Niesen FH, Berglund H, Vedadi M. The use of differential scanning fluorimetry to detect ligand interactions that promote protein stability. *Nat Protoc*. 2007;2:2212-2221.
27. Naoe Y, Arita K, Hashimoto H, Kanazawa H, Sato M, Shimizu T. Structural characterization of calcineurin B homologous protein 1. *J Biol Chem*. 2005;280:32372-32378.
28. Ikura M. Calcium binding and conformational response in EF-hand proteins. *Trends Biochem Sci*. 1996;21:14-17.
29. Chin D, Means AR. Calmodulin: a prototypical calcium sensor. *Trends Cell Biol*. 2000;10:322-328.
30. Ammar YB, Takeda S, Hisamitsu T, Mori H, Wakabayashi S. Crystal structure of CHP2 complexed with NHE1-cytosolic region and an implication for pH regulation. *EMBO J*. 2006;25:2315-2325.
31. Scheuermann TH, Padrick SB, Gardner KH, Brautigam CA. On the acquisition and analysis of microscale thermophoresis data. *Anal Biochem*. 2016;496:79-93.
32. Wiseman T, Williston S, Brandts JF, Lin LN. Rapid measurement of binding constants and heats of binding using a new titration calorimeter. *Anal Biochem*. 1989;179:131-137.

33. Kemmer G, Keller S. Nonlinear least-squares data fitting in excel spreadsheets. *Nat Protoc*. 2010;5:267-281.
34. Majorek KA, Kuhn ML, Chruszcz M, Anderson WF, Minor W. Double trouble-Buffer selection and His-tag presence may be responsible for nonreproducibility of biomedical experiments. *Protein Sci*. 2014;23:1359-1368.
35. Rochetteegly C, Stussigaraud C. Selective detection of calmodulin in polyacrylamide gels by double staining with coomassie blue and silver. *Electrophoresis*. 1984;5:285-288.
36. Wittig I, Schagger H. Features and applications of blue-native and clear-native electrophoresis. *Proteomics*. 2008;8:3974-3990.
37. Kroeger T, Frieg B, Zhang T, et al. EDTA aggregates induce SYPRO orange-based fluorescence in thermal shift assay. *PLoS ONE*. 2017;12.
38. Elbers D, Scholten A, Koch KW. Zebrafish recoverin isoforms display differences in calcium switch mechanisms. *Front Mol Neurosci*. 2018;11.
39. Matulis D, Lovrien R. 1-anilino-8-naphthalene sulfonate anion-protein binding depends primarily on ion pair formation. *Biophys J*. 1998;74:422-429.
40. Gasymov OK, Glasgow BJ. ANS fluorescence: potential to augment the identification of the external binding sites of proteins. *Biochimica Et Biophysica Acta-Proteins and Proteomics*. 2007;1774:403-411.
41. Huynh K, Partch CL. Analysis of protein stability and ligand interactions by thermal shift assay. *Curr Protoc Protein Sci*. 2015;79:28 29 21-14.
42. Cornish-Bowden A. Enthalpy—entropy compensation: a phantom phenomenon. *J Biosci*. 2002;27:121-126.
43. Wieprecht T, Apostolov O, Beyermann M, Seelig J. Thermodynamics of the alpha-helix-coil transition of amphipathic peptides in a membrane environment: Implications for the peptide-membrane binding equilibrium. *J Mol Biol*. 1999;294:785-794.
44. Gill SJ, Wadso I. An equation of state describing hydrophobic interactions. *Proc Natl Acad Sci USA*. 1976;73:2955-2958.
45. Bhattacharya S, Bunick CG, Chazin WJ. Target selectivity in EF-hand calcium binding proteins. *Biochimica Et Biophysica Acta-Mol Cell Res*. 2004;1742:69-79.
46. Andrade J, Zhao H, Titus B, Timm Pearce S, Barroso M. The EF-hand Ca2+-binding protein p22 plays a role in microtubule and endoplasmic reticulum organization and dynamics with distinct Ca2+-binding requirements. *Mol Biol Cell*. 2004;15:481-496.
47. Timm S, Titus B, Bernd K, Barroso M. The EF-hand Ca2+-binding protein p22 associates with microtubules in an N-Myristoylation-dependent manner. *Mol Biol Cell*. 1999;10:3473-3488.

SUPPORTING INFORMATION

Additional supporting information may be found online in the Supporting Information section.

How to cite this article: Liang S, Fuchs S, Mymrikov EV, et al. Calcium affects CHP1 and CHP2 conformation and their interaction with sodium/proton exchanger 1. *The FASEB Journal*. 2020;00:1–14. https://doi.org/10.1096/fj.201902093R